Synthesis and Density Functional Theory Studies of
Octakis(propyl)porphyrazine and its Zn(II) Complex

M.K. Mongale[1], D.A. Isabirye[1,*], M.M. Kabanda[2], T.O. Aiyelabola[1,3] and E.E. Ebenso[2]

[1]Department of Chemistry, School of Mathematical and Physical Sciences, North-West University (Mafikeng Campus), Private Bag X2046, Mmabatho 2735, South Africa
[2]Material Science Innovation & Modelling (MaSIM) Research Focus Area, Faculty of Agriculture, Science and Technology, North-West University (Mafikeng Campus), Private Bag X2046, Mmabatho 2735, South Africa
[3]Department of Chemistry, Obafemi Awolowo University, Ile-Ife, Nigeria

*Corresponding author: E-mail: david.isabirye@nwu.ac.za

Metalloporphyrazine 2,3,7,8,12,13,17,18-*octakis*(propyl)porphyrazine Zn(II) was synthesized and characterized using elemental analysis, IR, ^{1}H NMR and UV-visible spectroscopy. The kinetics of the incorporation of Zn(II) into the free base 2,3,7,8,12,13,17,18-*octakis*(propyl) porphyrazine was also investigated. Quantum chemical calculations (utilizing B3LYP/6-31G(d,p) method) was carried out on the free base and its Zn(II) complex to determine their electronic and geometric properties. Time-dependent Density Functional theory (TDDFT) approach was utilized for the analysis of the UV-visible spectra. The results indicated that both the experimental and theoretical results were in reasonable agreement. This showed that metallation and alkylation respectively had significant influence on the molecular and electronic properties of the porphyrazine moiety. It was proposed that the peripheral substituent, cavity size and the size of the metal ion incorporated are the main factors that determine metallation rate and consequently reactivity of the metalloporphyrazine complex.

Keywords: Porphyrazine derivatives, Alkylation, Metalloporphyrazine, Macrocyclization, Mulliken atomic charges.

INTRODUCTION

Porphyrazine (Pz) derivatives are used for various applications including dye-sensitized solar cells, semi-conductors, as biomedical agents in photodynamic therapy, gas sensors, and as non-linear optics [1-5]. These wide applicability of porphyrazine derivatives lies mainly in the properties of its molecules, such as high symmetry, planarity and electron delocalization [6-9]. There is an increase in the search for porphyrazine derivatives with important biological, photochemical and photophysical activities because of their wide applicability and uses. In most of the cases, the study on metallocyclicporphyrazine compounds involves the synthesis of new porphyrazine derivatives and the study of the effects of metallation on the metal free porphyrazine ligand. Theoretical methods are also increasingly applied to elucidate the molecular properties of these compounds [6-9]. Such studies provide information which might be utilized for possible modification of porphyrazines for various applications.

Our group had previously reported on the synthesis, characterization, kinetic studies of metallation and redox activities for some macrocyclic compounds [10]. In continuation

of our work on the effect of the size of the metal ion incorporated within the central cavity of 2,3,7,8,12,13,17,18-*octakis*-(propyl)porphyrazine, the incorporation of Zn(II) ion was considered. This was as a result of its comparable size with magnesium and its biological importance [11]. Therefore the objectives of this work was to synthesize, characterize and kinetics of the formation of 2,3,7,8,12,13,17,18-*octakis*-(propyl)PzZn(II) compound [oct(pr)PzZn(II)]. Compare *via* theoretical means the effects of Zn(II) metallation on the molecular and spectroscopic properties of the metal free oct(pr)Pz. Also to investigate the effect of alkylation on the molecular properties of 2,3,7,8,12,13,17,18-*octakis*(propyl)Pz ligand [oct(pr)Pz] using density functional theory. The schematic representations of the studied compounds are shown in Fig. 1.

EXPERIMENTAL

All the reagents used were obtained from UnivAR, Saarchem and Merck Chemical (Pty) Ltd. Solvents used for reactions were distilled prior to use: dichloromethane (from CaH_2); dimethylformamide (pre-dried from barium oxide) distilled in alumina; tetrahydrofuran (THF) was heated over sodium
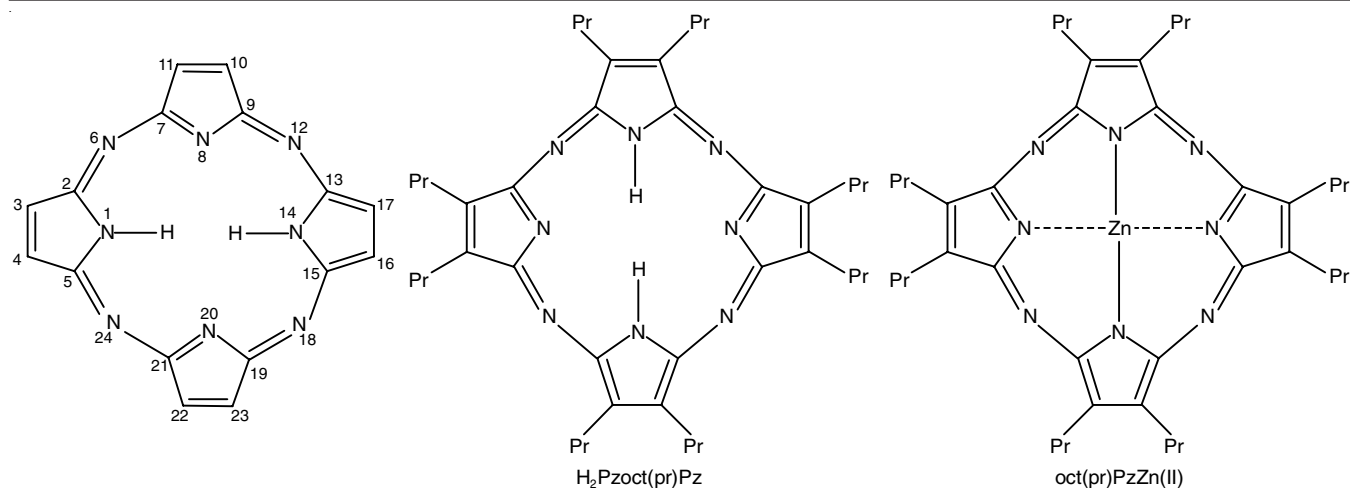
Fig. 1. Schematic representations of the studied compounds. The numbering of the atoms necessary for discussion is shown in the H_2Pz structure

benzophenone under nitrogen (N_2) until a blue colour persisted with subsequent distillation under nitrogen prior to use.

Infrared spectra were recorded on a Nicolet 410 impact Fourier transform infrared spectrophotometer using nujol and potassium bromide (KBr) cells. The range of interest was between 4000 and 500 cm^{-1}. The ultraviolet-visible absorption spectra were measured in a 1 cm quartz cell using a Varian Cary 50 ultraviolet-visible spectrophotometer. The ^1H NMR and ^{13}C NMR spectra of the compounds were recorded on a Varian-Gemini-300 (300 MHz) spectrometer in $CDCl_3$. The micro analysis was done at the University of Botswana Micro-analytical services.

Synthesis of compounds: Syntheses of the free base oct(pr)Pz and oct(pr)PzMg(II) was as reported previously by Isabirye and co-workers [10].

Preparation of oct(pr)PzZn(II): Zinc(II) acetate (25 mg, 0.1 mmol) was added to a solution of porphyrazine base, oct(pr)Pz (90 mg, 0.1 mmol) in dimethyl formamide. The mixture was shaken vigorously until a uniform solution was obtained. The solution was then refluxed under nitrogen controlled atmosphere for one hour after which it was cooled and concentrated on a rotary evaporator to give dark green oil. Addition of dichloromethane: tetrahydrofuran and stirring, gave a brown solid. The product was precipitated from dichloromethane:methanol as a greenish solid (47 mg, 63 %). ^1H NMR ($CDCl_3$): 1.86 (t, 24H, $J = 7.7$ Hz, CH_3), 3.98 (q, 16H, $J = 7.7$ Hz, $CH_2CH_2CH_3$). Anal. calcd. for $C_{40}H_{56}N_8Zn$: C, 67.3; H, 7.8; N, 15.7 Found: C, 67.0; H, 8.2; N, 16.5.

Computational details: The optimized geometries were obtained utilizing density functional theory (DFT) method with the B3LYP functional. The 6-31G(d) basis set was selected for all the calculations as a compromise between computational affordability and results meaningfulness. The B3LYP/6-31G(d) method has been found to provide adequate description of the geometry and other molecular properties of different macrocyclic molecules [6,7,9,12,13]. The vertical excitation energies were calculated by means of the time-dependent density functional theory (TDDFT) method. Time-dependent density functional theory has been successfully applied in the prediction of the electronic absorption spectra of a number of different macrocycles [12-16]. Moreover, the time-dependent DFT

(TDDFT) methodology provides a good compromise between the desired accuracy and the computational demand [17-19].

Frequency calculations were performed on optimized geometries to establish the nature of the stationary point on the potential energy surface. The geometry optimizations were performed by using the Spartan program [20,21] while the UV-visible spectra were analyzed by using the Gaussian program [22-24].

RESULTS AND DISCUSSION

In order to identify the contributions of zinc and to emphasize the photoemission spectral changes induced by the replacement of the two central hydrogen atoms by zinc, the spectra of oct(pr)PzZn(II) was compared with that of free base, oct(pr)Pz.

NMR spectra: The ^1H NMR spectrum of oct(pr)PzZn(II) closely resembled that of the free base. The success of metallation was however confirmed by the absence of the N-H signal present in the spectrum of the free base at -2.11 ppm [25,26]. No significant difference was observed in the ^{13}C NMR for both the free base and complex.

Ultraviolet visible spectrum: It has been shown that for non-metallated porphyrazines (D_{2h} symmetry), the UV-visible spectra show two lower energy split Q-bands at 550-700 nm and a higher energy Soret (B) band at 300-400 nm, which are assigned to $a_u \rightarrow b_{2g}$ (Qx), $a_u \rightarrow b_{3g}$ (Qy) and $b_{1u} \rightarrow b_{2g}$ (Bx), $b_{1u} \rightarrow b_{3g}$ (By) transitions (Fig. 2). These transition bands are assigned to excitations from the two highest-occupied molecular orbitals (HOMO) (a_{1u} and a_{2u}) into lowest unoccupied molecular orbitals (LUMO), e_g) [27]. On the other hand, metallated porphyrazines exhibit two intense $\pi \rightarrow \pi^*$ absorbance: a low energy Q band that may be accompanied by a slight higher energy shoulder and a higher energy B band [28]. For metalated porphyrazines, the symmetry of the chromophore is D_{4h} with the two LUMOs b_{2g} and b_{3g} giving rise to a two-fold degenerate e_g level resulting to unsplit Q and B absorptions bands associated with transitions $a_{1u} \rightarrow e_g$ and $a_{2u} \rightarrow e_g$ [29].

The spectrum of metal free oct(pr)Pzbase (Fig. 3) showed Q-band and B-band, both of which were attributed to allowed $\pi \rightarrow \pi^*$ transitions [12,13]. The Q band in the free base was splitted and had significant peaks at 626 and 558 nm, corresponding to a splitting of 68 nm. The spectrum of oct(pr)PzZn(II)
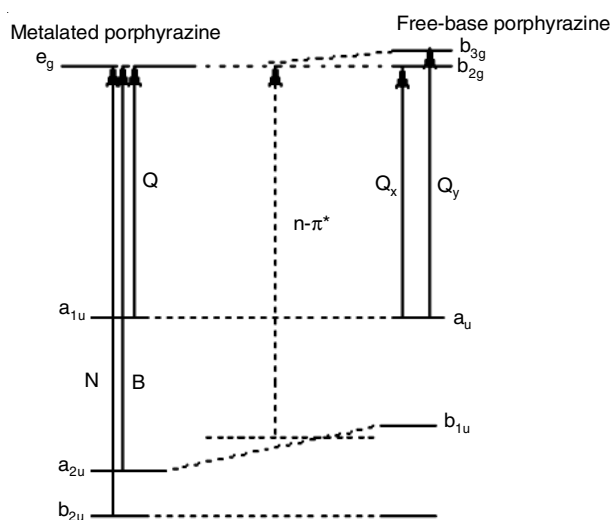
Metalated porphyrazine

Free-base porphyrazine

Fig. 2. Electronic transitions in the visible and close UV regions of metalated and non-metalatedporphyrazines

(Fig. 4) exhibited a single Q-band at 597 nm. These results are in accord with established literature and suggest that the free base oct(pr)Pz had D_{2h} symmetry while oct(pr)PzZn(II) had D_{4h} symmetry [10,26,30]. The B band in metal free oct(pr)Pz was observed at 340 nm. However on coordination it was shifted to 348 nm, which indicated coordination of the Zn(II) ion. The shoulder bands reported for oct(pr)PzZn(II) and oct(pr)Pz base are attributable to the $n \rightarrow \pi^*$ transition of the non-bonding electrons on the meso-nitrogen atoms of the macrocycle [28]. Further evidence of coordination was given by the appearance of a band at 442 nm, absent in that of the free base but observed fot the complex, assigned as metal ligand charge transfer.

Infrared: The absence of N-H stretching band in the infrared spectrum of the complex, which was present in free base, served as evidence for coordination Table-1. A band observed at 522 cm^{-1} absent in the spectrum of the free base but present in that of of the complex oct(pr)PzZn(II)ascribed to the ν(Zn-N) stretching band corroborates this further [31]. Shifts in the C=C band in the free base in 1640-1608 cm^{-1} region in the coordinated complex further supports the incorporation of the Zn(II) ion in the central cavity of oct(pr)Pz. Relevant infrared frequencies for the metallated and free porphyrazines are shown in Table-2.
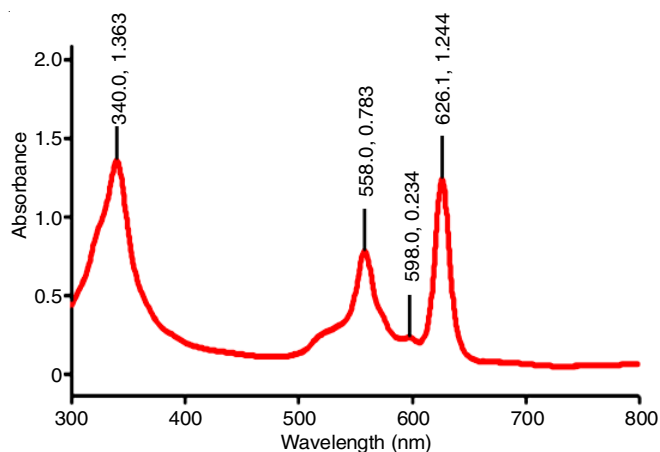

Fig. 3. UV-visible spectrum of 2,3,7,8,12,13,17,18-*octakis*(propyl)-porphyrazine base in dimethylformamide
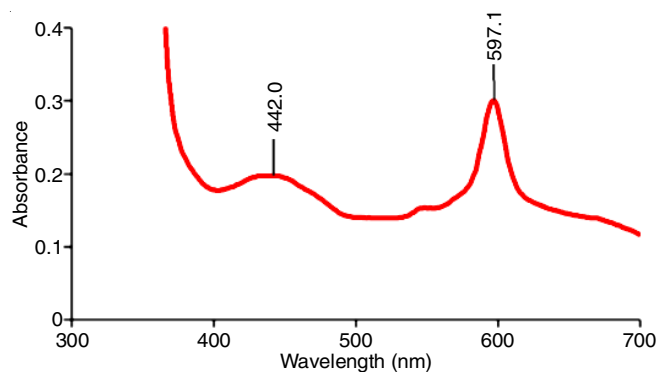

Fig. 4. UV-visible spectrum of 2,3,7,8,12,13,17,18-*octakis*(propyl-porphyrazinato)Zn(II) in dimethylformamide

TABLE-1
KEY INFRARED FREQUENCIES FOR METALLATED
PORPHYRAZINE AND PORPHYRAZINE FREE BASE

Complex	Band (cm^{-1})	Assignment
oct(pr)Pz base	3021	ν(N-H)
	2928-2851	ν(CH$_2$, CH$_3$)
	1464	ν(C-H)
	1209	ν(C=C)
	723	ν(C-H)
oct(pr)PzZn(II)	3055	ν(C-H) aromatic
	2925-2854	ν(CH$_2$, CH$_3$)
	1640	ν(C=C)
	522	ν(Zn-N)

TABLE-2
RATE CONSTANT (K, 25 °C) AND ACTIVATION
ENERGY (E$_a$) FOR THE KINETIC REACTIONS

Compound	K (M^{-1} s^{-1})
oct(pr)PzZn(II)^a	0.40
oct(pr)pzZn(II) ^{a}	4.53
oct(pr)PzCo(II) [Ref. 10]	2.70
oct(pr)PzCu(II) [Ref. 10]	2.81
^{a}Formed *via* dinuclear complex	

Metallation: The rate of incorporation of Zn(II) ion into the central cavity of oct(pr)Pz free base and oct(pr)pzMg(II) was studied and the results obtained are shown in Table-2. Preliminary repetitive scanning of the ultraviolet spectral region during the reaction gave well defined isosbestic points at 475, 596 and 625 nm (Fig. 5). The plots of 1/[A] *versus* time were linear, suggesting second order kinetics. The results
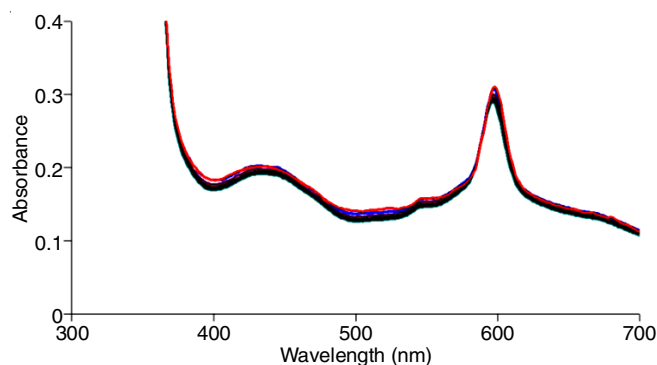

Fig. 5. Spectral changes during the reaction of 2,3,7,8,12,13,17,18-*octakis*-(propylporphyrazinato)Mg(II) (5 × 10^{-6} M) and zinc acetate (1 × 10^{-2} M) in dimethylformamide at 24 °C at 15 min

indicated that the rate of incorporation of Zn(II) into oct(pr)Pz free base was faster than that of oct(pr)PzMg(II) (Table-2). This indicates that incorporation of zinc ion directly into the free base is the more favourable pathway for its incorporation.

A comparison of the rate of coordination of Zn(II) ion into the free base with those of previously reported divalent metal ions indicated an incorporation order of Zn > Cu > Co. This arrangement indicates that the size of the incorporated metal is a function of the rate of incorporation. It is however not consistent with that obtained by Hambright and Crock for porphyrins [32]. We propose that such difference may be as a result of the cavity size. In porphyrazines macrocyclization occurs around magnesium, in contrast to that of porphyrins, before demetallation to obtain the free base [33,34]. It is suggested that the size of magnesium may define the central cavity to some extent in porphyrazine. Consequently it can be inferred therefore that as Zn(II) has a relatively comparable size to that of magnesium, there will be less strain on the core of the macrocycle and better fit of the metal ion, leading to faster rate of incorporation compared to the earlier reported divalent metal ions. Similar correlations was obtained by Funahashi and co-workers [35] in which there was faster rate of incorporation for Zn(II) compared to Cd(II) ion. These results point to the fact that although the cores of these macro-

cycles are flexible, they are to an extent defined. Consequently showing their ability to selectively incorporate metal ions and hence their usage as analytical tools for the determination of trace metals. The observed MLCT band for the spectral changes indicated probable electron donating tendency of the ligand, suggestive of ligand based oxidation process as probable first redox activity for the complex [10,30].

Quantum chemical studies

Geometric and electronic parameters: The optimized geometries of the non-alkylated free porphyrazine, free base oct(pr)Pz and metalloporphyrazine oct(pr)PzZn(II) are shown in Fig. 6. For the purpose of comparative studies, calculated result on non-alkylated porphyrazine (H_2Pz) has also been performed to investigate the influence of the alkyl chains on the properties of the porphyrazine moiety. The geometric parameters (*i.e.*, bond lengths and bond angles) for all the structures are shown in Table-3. A comparison of the bond lengths and bond angles for non-alkylated free porphyrazine and free oct(pr)Pz suggests that alkylation has minimal influence on the properties of the free porphyrazine base. However, a comparison of the bond lengths and bond angles for free oct(pr)Pz and the oct(pr)PzZn(II), suggests that metallation has significant influence on the geometry of the porphyrazine.
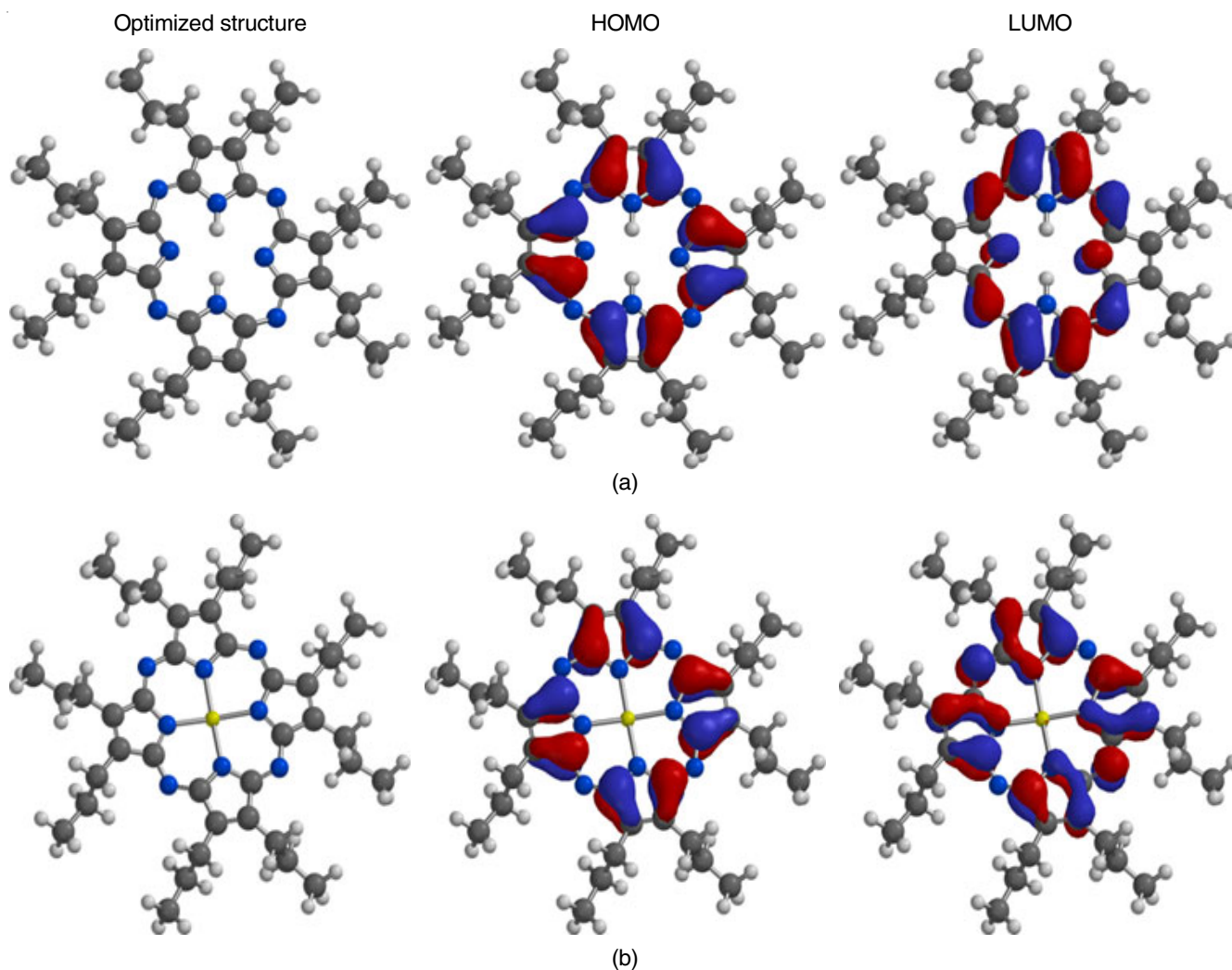

Fig. 6. Optimised structure and the corresponding HOMO and LUMO for (a) *octakis*(propyl)Pz and (b) for *octakis*(propyl)PzZn(II)

TABLE-3
SELECTED BOND LENGTHS (Å) AND BOND ANGLES (°) FOR
PORPHYRAZINE DERIVATIVES AND ITS COMPLEX FORM

Geometric parameter	H₂Pz	oct(pr)Pz	oct(pr)PzZn(II)
Bond length (Å)			
N1-C2	1.372	1.372	1.367
N1-C5	1.371	1.371	1.367
C2-C3	1.454	1.454	1.466
C3-C4	1.378	1.378	1.372
C4-C5	1.453	1.454	1.466
C2-N6	1.324	1.323	1.335
N6-C7	1.338	1.338	1.335
C7-N8	1.361	1.362	1.367
N8-C9	1.362	1.362	1.367
C7-C11	1.475	1.476	1.466
C9-C10	1.475	1.475	1.466
C10-C11	1.363	1.363	1.372
C9-N12	1.338	1.338	1.335
N12-C13	1.323	1.323	1.335
C13-N14	1.371	1.372	1.367
N14-C15	1.372	1.371	1.367
C13-C17	1.453	1.454	1.466
C15-C16	1.454	1.454	1.466
C16- C17	1.378	1.378	1.372
C15-N18	1.324	1.323	1.335
N18-C19	1.338	1.338	1.335
C19-N20	1.361	1.361	1.367
N20-C21	1.362	1.362	1.367
C19-N23	1.476	1.476	1.466
C21-C22	1.476	1.476	1.466
C22-C23	1.363	1.363	1.372
C21-N24	1.338	1.338	1.335
N24-C5	1.323	1.323	1.335
Bond angle (°)			
C2N1C5	110.5	110.5	107.8
C2N6C7	123.1	123.1	124.0
C7N8C9	105.0	105.0	107.8
C9N12C13	123.1	123.1	124.0
C13N14C15	110.5	110.5	107.8
C15N18C19	123.1	123.1	124.0
C19N20C21	105.0	105.0	107.8
C21N24C5	123.1	123.1	124.0

The changes observed on metallation in the bond lengths are less than 0.2Å and depend on the type of the bond considered. The bond lengths (Å) of C2-C3, C4-C5, C13-C17, C15-C16 increased by 0.012 Å; the bond lengths (Å) of N6-C7, C9-N12, N18-C19 and C21-N24 bonds decreased by 0.003; the bond lengths (Å) of N1-C2, N1-C5, C13-N14 and N14-C15 bonds (*i.e.*, the bond on the protonated pyrrole in the free porphyrazine) decreased by ≈ 0.005 while the bond length of C7-N8, N8-C9, C19-N20 and N20-C21 bonds (*i.e.*, the bond on the non-protonated pyrrole rings in the free Pz) increase by ≈ 0.005 Å. The lengths of the C10-C11 and C22-C23 bonds increase by 0.009 Å. The bond length of C2-N6, N12-C13, C15-N18 and N24-C5 increases by 0.012 Å while the bond lengths of C7-C11, C9-C10, C19-N23 and C21-C22 decreases by ≈ 0.009 Å. The bond lengths of C3-C4 and C16-C17 decrease by 0.003 Å. These observed elongation and shortening of bond lengths points to the necessary deformation and rearrangements of the macrocycle essential for effective coordination of the metal ion. This is in agreement with previous studies [10,32]. The changes observed in the bond angles also depends on the type of the angle considered. The C2N1C5 and C13N14C15 bond angles (*i.e.*, the bond angles on the pyrrole rings that are

protonated in the free porphyrazine base) decreases by 2.7° on metallation while the C7N8C9 and C19N20C21 angles (*i.e.*, the bond angles on the pyrrole rings that are non-protonated in the free porphyrazine base) increases by 2.8°. The C2N6C7, C9N12C13, C15N18C19 and C21N24C5 angles increase by 0.9°. These further corroborate the deformation of the macrocycle. A comparison of the N1H1···H14N14 and the N8···N20 separation distances between the H2Pz and oct(pr)Pz shows that on alkylation, the distance between the two central hydrogen atoms decreases from 1.965 to 1.962 Å and the N8···N20 decreased from 3.824 to 3.820 Å, and suggestive of the flexible nature of the macrocyclic core [25].

The Mulliken atomic charges of the core porphyrazine fragment for the three compounds are listed in Table-4 and the results show that they are affected by both alkylation and metallation. A comparison of the Mulliken atomic charges on the atoms of the non-alkylated free porphyrazine and the corresponding atoms on the free oct(pr)Pz suggests that the charge on all the atoms become more negative on alkylation, resulting from the electron donating effect due to the alkyl chains. A comparison of free oct(pr)Pz base and oct(pr)PzZn(II) suggests that Zn metallation of the porphyrazine base decreases the Mulliken atomic charge of N1 and N14 by 0.014e and C7, C9, C19 and C21 by 0.022; increases the Mulliken atomic charges of N8 and N20 by ≈ -0.053e and C2, C13 and C15 by 0.021-0.023e. The Mulliken atomic charge on meso-nitrogen atoms (*i.e.*, N6, N12, N18 and N24 atoms) show no significant influence from metallation, suggesting that the atoms whose Mulliken atomic charge changes most are those directly bonding to the Zn metal or in the vicinity of the Zn-N bonds.

TABLE-4
MULLIKEN ATOMIC CHARGES ON THE ATOMS OF INTEREST
FOR THE STUDIED PORPHYRAZINE DERIVATIVES

Atom	H₂Pz	oct(pr)Pz	oct(pr)PzZn(II)
N1	-0.705	-0.731	-0.717
C2	0.523	0.505	0.483
N6	-0.553	-0.572	-0.572
C7	0.485	0.462	0.483
N8	-0.639	-0.664	-0.717
C9	0.484	0.461	0.483
N12	-0.553	-0.572	-0.571
C13	0.524	0.505	0.482
N14	-0.705	-0.731	-0.717
C15	0.523	0.505	0.484
N18	-0.553	-0.572	-0.571
C19	0.485	0.462	0.483
N20	-0.639	-0.663	-0.717
C21	0.484	0.462	0.484
N24	-0.553	-0.572	-0.572

The reactivity trend of free base and the metallated porphyrazines was also studied by considering their frontier molecular orbitals (*i.e.*, the highest occupied molecular orbital (HOMO) and the lowest unoccupied molecular orbital (LUMO)) and the corresponding energies, *i.e.*, E_{HOMO}, E_{LUMO} and ΔE, where ΔE is the energy difference between E_{HOMO} and E_{LUMO}. E_{HOMO} describes the electron donating ability of a given molecule, E_{LUMO} describes the electron accepting ability of a molecule and ΔE describes the reactivity tendency of a given molecule [27]. The highest occupied molecular orbital of the studied

TABLE-6
CALCULATED AND EXPERIMENTAL ABSORPTION PARAMETERS OF H₂Pz, oct(pr)Pz AND oct(pr)PzZn

Structure	Absorption parameters				
	Calculated			Experimental	
	Wavelength (nm)	Oscillator strength*	Excitation energy (eV)	Wavelength (nm)	Absorbance**
H₂Pz	521.40	0.1229	2.34	–	–
	492.00	0.1248	2.52	–	–
	395.14	0.0994	3.14	–	–
	384.15	0.0345	3.23	–	–
oct(pr)Pz	538.47	0.2031	2.30	558.0	0.783
	508.61	0.1994	2.44	598.0	0.234
	443.81	0.0344	2.79	626.1	1.244
	433.56	0.0057	2.86		
	364.47	0.0946	3.40	340.0	1.363
oct(pr)PzZn	519.72	0.2236	2.39	597.1	0.300
	411.80	0.0026	3.01	442.0	0.197
	371.53	0.1017	2.41	348.0	0.264

*Some parameters have oscillator strength less than 0.01 are excluded.
**The experimental absorbance measurements were performed in dimethylformamide solution (DMF).

compounds are shown in Fig. 3 and the E_{HOMO}, E_{LUMO} and ΔE values are reported in Table-5. The results for the different compounds suggest that both alkylation and metallation have significant influence on the energy level of the molecular orbitals of porphyrazines. On alkylation, E_{HOMO} increases (*i.e.*, electron donating ability increases) and the energy gap decreases (*i.e.*, reactivity tendency increases) while E_{LUMO} increases (*i.e.*, electron accepting ability decreases). Metallation on the other hand, increases the electron donating and decreases the electron accepting and reactivity tendency of porphyrazines.

TABLE-5
ENERGY (eV) OF HOMO, LUMO AND ΔE AND DIPOLE
MOMENT OF PORPHYRAZINE DERIVATIVES

Quantum chemical parameter	H₂Pz	oct(pr)Pz	oct(pr)PzZn(II)
E_{HOMO}	-5.82	-5.30	-5.27
E_{LUMO}	-3.19	-2.76	-2.67
ΔE (eV)	2.63	2.54	2.60
Dipole moment (debye)	0.00	0.65	0.83

Two Q bands at 538 and 508 nm, equal to a splitting of 29 nm, was predicted by TDDFT method for the free base oct(pr)Pz. In case of the oct(pr)PzZn(II) complex however, a single peak was obtained for the Q band at 519 nm and a shoulder band at 411 nm. The B band in metal free oct(pr)Pz base at 364 nm was shifted to 371 nm in the complex. These results are in reasonable agreement with those obtained experimentally; a comparison for both is shown in Table-6. These results suggests that the free base oct(pr)Pz had D₂ₕ symmetry while oct(pr)PzZn(II) had D₄ₕ symmetry [10,26,30].

Conclusion

It was concluded that theoretical studies may be of assistance in propounding the structure and reactivity of these macrocyclic compounds. As such they may be of immense assistance for their experimental studies. It was further concluded that although the core of the porphyrazine free base may be flexible it is to an extent defined by the metal ion incorporated during macrocyclization. Therefore metallation rate for these macrocycles is not only a function of the peripheral functionalities but also of the cavity size and the size of the metal ion to be incorporated.

REFERENCES

1. B. Cosimelli, G. Roncucci, D. Dei, L. Fantetti, F. Ferroni, M. Ricci and D. Spinelli, *Tetrahedron*, **59**, 10025 (2003).
2. P. Kubát and J. Mosinger, *J. Photochem. Photobiol. Chem.*, **96**, 93 (1996).
3. G. Li, S.K. Pandey, A. Graham, M.P. Dobhal, R. Mehta, Y. Chen, A. Gryshuk, K. Rittenhouse-Olson, A. Oseroff and R.K. Pandey, *J. Org. Chem.*, **69**, 158 (2004).
4. A.G. Montalban, W. Jarrell, E. Riguet, Q.J. McCubbin, M.E. Anderson, A.J.P. White, D.J. Williams, A.G.M. Barrett and B.M. Hoffman, *J. Org. Chem.*, **65**, 2472 (2000).
5. W. Freyer and S. Flatau, *Tetrahedron Lett.*, **37**, 5083 (1996).
6. X. Zhang, Y. Zhang and J. Jiang, *J. Mol. Struct. THEOCHEM*, **673**, 103 (2004).
7. X. Zhang and J. Jiang, *J. Electron Spectrosc. Relat. Phenom.*, **142**, 145 (2005).
8. X. Zhang, N. Kobayashi and J. Jiang, *Spectrochim. Acta A Mol. Biomol. Spectrosc.*, **64**, 526 (2006).
9. Z. Liu, X. Zhang, Y. Zhang, R. Li and J. Jiang, *Spectrochim. Acta A Mol. Biomol. Spectrosc.*, **65**, 467 (2006).
10. D.A. Isabirye, F.M. Mtunzi and T.O. Aiyelabola, *Dyes Pigments*, **109**, 214 (2014).
11. N.N. Greenwood and A. Earnshaw, Chemistry of the Elements, Pergamon Press, Oxford (1984).
12. E. Gonca, Y. Köseoglu, B. Aktas and A. Gül, *Polyhedron*, **23**, 1845 (2004).
13. H. Akku and A. Gül, *Transition Met. Chem.*, **26**, 689 (2001).
14. V.N. Nemykin, R.G. Hadt, R.V. Belosludov, H. Mizuseki and Y. Kawazoe, *J. Phys. Chem. A*, **111**, 12901 (2007).
15. A. Baccouche, B. Peigné, F. Ibersiene, D. Hammoutène, A. Boutarfaïa, A. Boucekkine, C. Feuvrie, O. Maury, I. Ledoux and H. Le Bozec, *J. Phys. Chem. A*, **114**, 5429 (2010).
16. G. Ricciardi, A. Rosa and E.J. Baerends, *J. Phys. Chem. A*, **105**, 5242 (2001).
17. D. Qi and J. Jiang, *J. Phys. Chem. A*, **115**, 13811 (2011).
18. K.A. Nguyen and R. Pachter, *J. Chem. Phys.*, **114**, 10757 (2001).
19. J. Mack, Y. Asano, N. Kobayashi and M.J. Stillman, *J. Am. Chem. Soc.*, **127**, 17697 (2005).
20. J. Fan, M. Seth, J. Autschbach and T. Ziegler, *Inorg. Chem.*, **47**, 11656 (2008).
21. Y. Shao, L.F. Molnar, Y. Jung, J. Kussmann, C. Ochsenfeld, S.T. Brown, A.T.B. Gilbert, L.V. Slipehenko, S.V. Levehenko, D.P. O'Neill, R.A. DiStasio Jr., R.C. Lochan, T.Wang, G.J.O. Beran, N.A. Besley, J.M. Herbert, C.Y. Lin, T. Van Voorhis, S.H. Chien, A. Sodt, R.P. Steele, V.A. Rassolov, P.E. Maslen, P.P. Korambath, R.D. Adamson, B. Austin, J. Baker, E.F.C. Byrd, H. Dachsel, R.J. Doerksen, A. Dreuw, B.D. Dunietz, A.D. Dutoi, T.R. Furlani, S.R. Gwaltney, A. Heyden, S. Hirata, C.P. Hsu, G. Kedziora, R.Z. Khalliulin, P.Klunzinger, A.M. Lee, M.S. Lee,

W.Z. Liang, I.Lotan, N. Nair, B.Peters, E.I. Proynov, P.A. Pieniazek, Y.M. Rhee, J. Ritchie, E. Rosta, C.D. Sherrill, A.C. Simmonett, J.E. Subotnik, H.L. Woodcock III, W.Zhang, A.T. Bell, A.K. Chakraborty, D.M. Chipman, F.J. Keil, A. Warshel, W.J. Hehre, H.F. Schaefer, J. Kong, A.I. krylov, P.M.W. Gill and M. Head-Gordon, *Phys. Chem. Chem. Phys.*, **8**, 3172 (2006).

22. J. Autschbach, T. Ziegler, S.J.A. van Gisbergen and E.J. Baerends, *J. Chem. Phys.*, **116**, 6930 (2002).

23. B. Le Guennic, W. Hieringer, A. Görling and J. Autschbach, *J. Phys. Chem. A*, **109**, 4836 (2005).

24. M.J. Frisch and H.B. Trucks, Schlegel, G.E. Scuseria, M.A. Robb, J.R. Cheeseman, J.A. Montgomery, T. Vreven, K.N. Kudin, J.C. Burant, J.M. Millam, S. S. Iyengar, J. Tomasi, V.Barone, B. Mennucci, M. Cossi, G. Scalmani, N. Rega, G.A. Petersson, H. Nakatsuji, M. Hada, M. Ehara, K.Toyota, R. Fukuda, J. Hasegawa, M. Ishida, T. Nakajima, Y. Honda, O. Kitao, H. Nakai, M. Klene, X. Li, J.E. Knox, H.P. Hratchian, J.B. Cross, C. Adamo, J. Jaramillo, R. Gomperts, R.E. Stratmann, O.Yazyev, A.J. Austin, R. Cammi, C. Pomelli, J.W. Ochterski, P.Y. Ayala, K. Morokuma, G.A. Voth, P. Salvador, J.J. Dannenberg, V.G. Zakrzewski, S. Dapprich, A.D. Daniels, M.C. Strain, O. Farkas, D.K. Malick, A.D. Rabuck, K. Raghavachari, J.B. Foresman, J.V. Ortiz, Q. Cui, A.G.

Baboul, S. Clifford, J. Cioslowski, B.B. Stefanov, G. Liu, A. Liashenko, P. Piskorz, I. Komaromi, R.L. Martin, D.J. Fox, T. Keith, M.A. Al-Laham, C.Y. Peng, A. Nanayakkara, M. Challacombe, P.M.W. Gill, B. Johnson, W. Chen, M.W. Wong, C. Gonzalez and J.A. Pople, GAUSSIAN 03, Gaussian, Inc., Pittsburgh, PA, USA (2003).

25. Y. Inada, Y. Sugimoto, Y. Nakano, Y. Itoh and S. Funahashi, *Inorg. Chem.*, **37**, 5519 (1998).

26. E. Gonca, *J. Coord. Chem.*, **66**, 1720 (2013).

27. T.F. Baumann, A.G.M. Barrett and B.M. Hoffman, *Inorg. Chem.*, **36**, 5661 (1997).

28. S. Sesalan and A.B. Gül, *Monatsh. Chem.*, **131**, 1191 (2000).

29. M.J. Cook and A. Jafari-Fini, *Tetrahedron*, **56**, 4085 (2000).

30. S. Tuncer, A. Koca, A. Gül and U. Avciata, *Dyes Pigments*, **92**, 610 (2012).

31. K. Nakamoto, Infrared and Raman Spectra of Inorganic and Coordination Compounds, 6th Ed. Wiley (2009).

32. P. Hambright and P. Chock, *J. Am. Chem. Soc.*, **96**, 3123 (1974).

33. T.P. Forsyth, D.B.G. Williams, A.G. Montalban, C.L. Stern, A.G.M. Barrett and B.M. Hoffman, *J. Org. Chem.*, **63**, 331 (1998).

34. S. Michel, B. Hoffman, S. Baum and A. Barrett, Progress in Inorganic Chemistry, John Wiley & Sons, New York, vol. 5, p. 473 (2001).

35. S. Funahashi, Y. Inada and M. Inamo, *Anal. Sci.*, **17**, 917 (2001).